Chaos, Solitons & Fractals 45 (2012) 125–130

Contents lists available at SciVerse ScienceDirect

Chaos, Solitons & Fractals

Nonlinear Science, and Nonequilibrium and Complex Phenomena

journal homepage: www.elsevier.com/locate/chaos

Negative correlation between power-law scaling and Hurst exponents in long-range connective sandpile models and real seismicity

Ya-Ting Lee [a], Chien-chih Chen [a,*], Chai-Yu Lin [b], Sung-Ching Chi [c]

[a] Graduate Institute of Geophysics, National Central University, Jhongli, Taoyuan 320, Taiwan, ROC
[b] Department of Physics, National Chung Cheng University, Ming-Hsiung, Chia-Yi 621, Taiwan, ROC
[c] Teaching Center of Natural Science, Minghsin University of Science and Technology, Xinfeng, Hsinchu 304, Taiwan, ROC

ARTICLE INFO

Article history:
Received 14 May 2011
Accepted 29 October 2011
Available online 3 December 2011

ABSTRACT

We propose a generic negative correlation between power-law scaling and Hurst exponents for size/magnitude data from real and synthetic earthquakes. The synthetic earthquakes were produced from a conceptual earthquake model, the long-range connective sandpile (LRCS) model. The LRCS model is a new modification of sandpile models that considers the random distant connection between two separated cells instead of neighboring cells. We calculated the Hurst exponent H and the power-law scaling exponent B for event size data in the LRCS model. We systematically explored the relationships between these two exponents (H and B) and conclusively obtained a negative correlation between H and B. We also found this negative correlation for real earthquake data registered in the Taiwan Central Weather Bureau (CWB) catalog. This negative correlation has not been demonstrated previously for real seismicity, although it has been frequently suggested.

1. Introduction

Sandpile dynamics and self-organized criticality (SOC) are exhibited by many natural and social phenomena, including earthquakes, forest fires, rainstorms, landscapes, drainage networks, stock prices, and traffic jams. Since Bak et al. [3,4] introduced the original nearest-neighbor sandpile model, a considerable amount of further research has adopted various numerical and analytical techniques to study modifications of the original sandpile model [24,9,22,16,2,13,18,7,8]. For example, *annealed random-neighbor sandpile* models were first proposed by Christensen and Olami [9] and were then extensively studied on a long-range connected (small-world) network by, for example, De Arcangelis and Herrmann [2], Lahtinen et al. [18], and Chen et al. [7,8].

We have previously proposed a *long-range connective sandpile* (LRCS) model that randomly introduces remote connections between two separated cells instead of nearest-neighboring cells [7,8,20,21]. In this paper, we calculate the Hurst exponent H of avalanche sizes and the power-law exponent B of the frequency-size distribution of avalanches in the LRCS model [7,8,20]. The relationships between the two exponents (H and B) show a strong dependence upon the calculated time scale, which is associated with the finite-size effect. By slightly removing the finite-size effect, we confirm the presence of a striking negative correlation between B- and H-values in the LRCS model. We further demonstrate a negative correlation between H and B in Taiwanese seismicity data.

2. Long-range connective sandpile (LRCS) models

The LRCS model differs from the original Bak-Tang-Wiesenfeld (BTW) sandpile model in the method of releasing grains to nearest-neighboring cells. For a square lattice of L by L cells, we throw sand randomly, one grain at a time, onto the grid. In the BTW sandpile model [3,4], once the total number of accumulated sand grains on a single cell reaches the threshold value of four, the sand grains

* Corresponding author. Tel.: +886 3 422 7151 65653; fax: +886 3 422 2044.
E-mail address: chencc@earth.ncu.edu.tw (C.-c. Chen).

0960-0779/$ - see front matter © 2011 Elsevier Ltd. All rights reserved.
doi:10.1016/j.chaos.2011.10.009

are redistributed onto the four adjacent cells (the nearest neighbors), or they are lost off the edge of the grid. Our LRCS model, however, releases toppled grains according to random connections within the whole L by L lattice. The modified rule of random internal connections is similar to the implementation of Watts and Strogatz [36]. For any particular cell, when the accumulated number of grains exceeds the threshold and redistribution occurs, one of the four original nearest-neighbor connections has a chance with the *long-range connective probability* P_c of redirecting to a randomly chosen distant cell so that the original nearest-neighbor connection is replaced by the randomly chosen cell, which may be far from the toppling cell. This implementation of releasing grains/energy to remote cells is reminiscent of plausible long-range effects in real earthquake fault systems ([7,8,20]; see also the text below).

We further assume that P_c depends strongly on the topographic change induced by the last event [8,20,21]. This relationship is defined as $P_c(t+1) = [\Delta Z(t)/\alpha L^2]^3$, where $\Delta Z(t)$ and L^2 represent the topographic change due to the last event and the system size, respectively. The coefficient α is similar to the normalization constant, which restricts the value of the connective probability P_c to between 0 and 1. The LRCS model can thus evoke a high value of P_c after a large avalanche, reflecting the fact that a more active earthquake fault system will have a higher probability of establishing long-range connections due to unstable fault activity, changes in pore-fluid pressure, or the dynamic triggering of seismic waves. For example, a larger earthquake generates more radiated energy carried by seismic waves, thus, is more capable of dynamically triggering remote tremors far away the main shock. In those remotely triggered cases, stress perturbation due to seismic waves is considered as the immediate cause of triggered events [34,28]. By using this self-adapted probability threshold P_c of the remote connection, the LRCS model demonstrates a state of *intermittent criticality* [27,25,6], in which the sandpile quasi-periodically approaches and retreats from the critical state. In the LRCS model with self-adapted P_c, the dynamic variable of the spatially averaged number of grains on the grid $\langle Z\rangle(t)$ ($\equiv \sum_{i=1}^{L^2} Z_i(t)/L^2$; blue line in Fig. 1) generally maintains increasing trends that are punctuated by large events (black bars in Fig. 1). The large fluctuation in $\langle Z\rangle(t)$ is an important feature that mimics the intermittent criticality [27,25,6,23,26,14].

A large avalanche is then followed by a period of quiescence and an approach back toward the critical state (Fig. 1) [8,20,21]. This process is similar to the dynamic process of an earthquake fault system, involving repetitive reloading of energy and rebuilding of correlation lengths toward criticality and the next major event [23,26,14]. The LRCS model proposed here could be called the *quarterly self-adaptive random-neighbor* BTW model, where

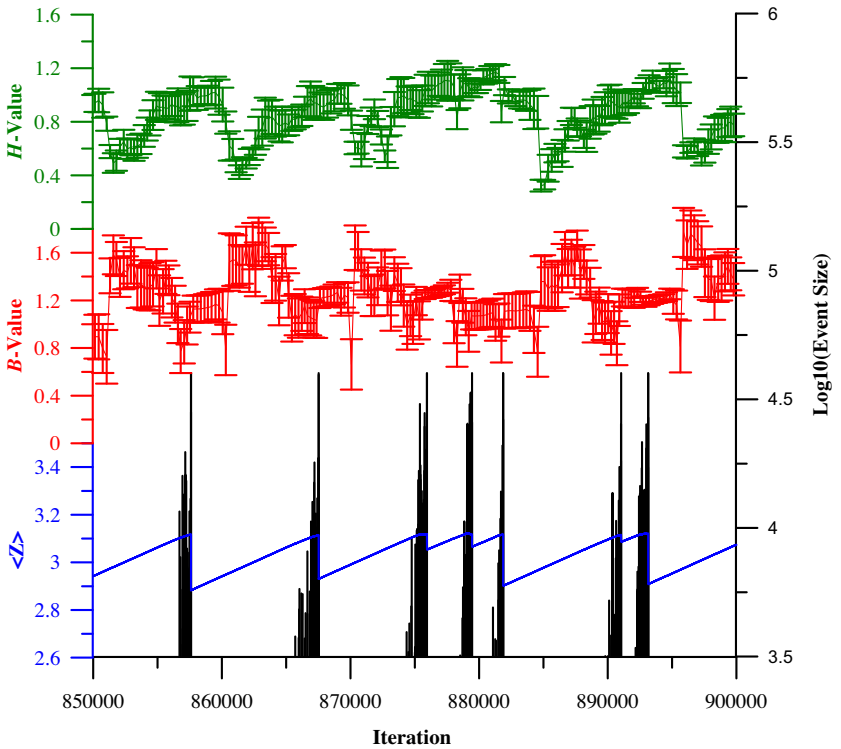

Fig. 1. Simulation of the LRCS model for a square lattice of 200 by 200 cells. The green and red lines represent the Hurst exponent H of avalanche sizes and the power-law exponent B of the frequency-size distribution, respectively. The B- and H-values are calculated from a 1000-event window that is shifted by 100 events to calculate the successive B- and H-values of the next window. The error bars show 95% confidence intervals. The blue line represents the dynamic variable $\langle Z\rangle(t)$ of the average topographic height of the LRCS model. The times of occurrence of avalanches with magnitudes greater than or equal to $10^{3.5}$ (black bars) are also shown. (For interpretation of the references to color in this figure legend, the reader is referred to the web version of this article.)

quarterly means that only one of the four nearest-neighbor connections is removed and redirected, and *self-adaptive* means that the long-range connective probability P_c is recalculated according to the topographic change induced by the last event. Note that although other random-neighbor versions of sandpile models have been proposed during the last two decades [24,9,22,16,2,13,18], none of them are self-adaptive in the sense of random connection probability. The self-adapted P_c plays a crucial role in the intermittency built into in the LRCS model. For more details about the LRCS model, we refer readers to our previous papers [8,20,21].

3. Relationship between *B*- and *H*-values for avalanches in the LRCS model

Here, we investigate temporal variations in the power-law exponent B of the frequency-size distributions and in the Hurst exponent H of avalanche sizes in LRCS models. To trace variations in B and H with respect to time, we used the sliding window technique. We selected various numbers of events (hereinafter called the window length) in a calculation window, ranging from 100 to 4000 events, to calculate the B- and H-values and then shifted the window by 10% of its length to calculate the successive B- and H-values of the next window. For example, if the window length was 500, we calculated B and H for 500 events and then shifted the window by 50 events to calculate the next values of B and H.

To calculate B, we applied the data binning technique proposed by Christensen and Moloney [10] to reduce the noise effect of large avalanches (i.e., the effect of finite statistics). We then performed a least-squares regression to fit the frequency-size distribution. The R/S analysis used to calculate H is briefly summarized below. The R/S analysis utilizes two factors: the range R, which is the difference between the maximum and minimum values of accumulated departure from the mean over a time series of length τ, and the standard deviation S over that time span. The rescaled range is defined as the ratio of R and S (i.e., R/S). The ratio R/S is closely described by the empirical relationship $(R/S)(\tau) = (\tau/2)^H$, where H is the so-called Hurst exponent.

Fig. 1 is an example of an LRCS model with a grid size of 200 by 200, demonstrating the temporal variations in B (red line) and H (green line). The B- and H-values were calculated for every 1000 events (i.e., a window length of 1000 events) (solid square in Fig. 2), and the window

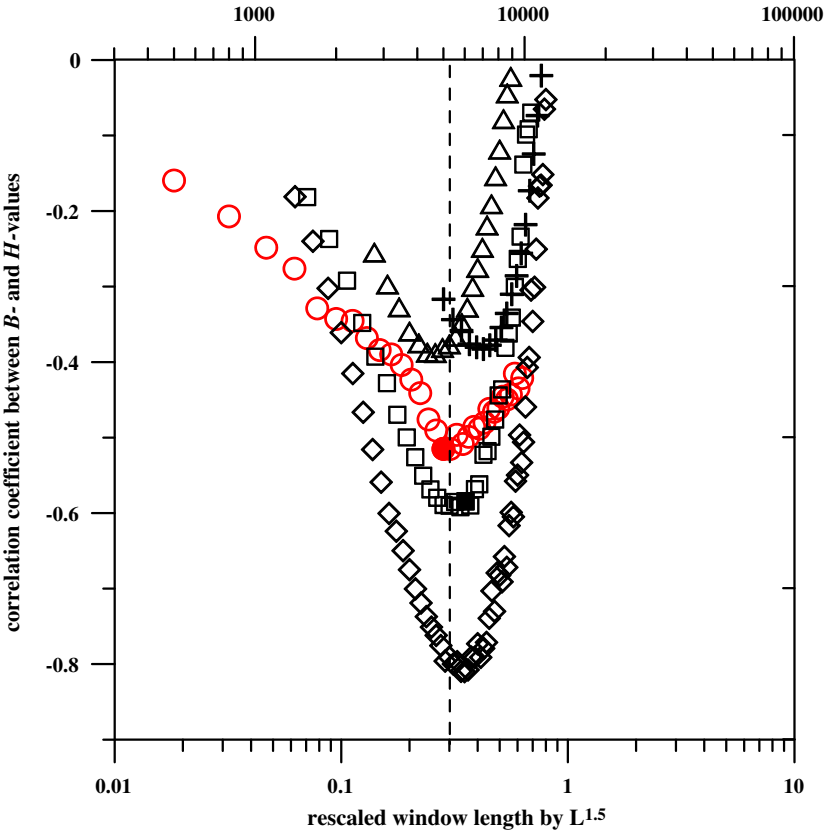

Fig. 2. Correlation coefficients between B- and H-values calculated with different window lengths for LRCS models. System sizes L range from 50 to 400 (crosses for $L = 50$; triangles for $L = 100$; squares for $L = 200$; diamonds for $L = 400$). The window lengths for the different grid sizes of LRCS models are rescaled by $L^{1.5}$. The vertical dashed line indicates the rescaled window length of 0.3. Red circles show the correlation coefficients between B- and H-values calculated with different window lengths (upper horizontal axis) for real earthquake data registered in the Taiwan CWB catalog. The solid black square and solid red circle represent the results obtained from the LRCS model in Fig. 1 and the CWB catalog in Fig. 4, respectively. (For interpretation of the references to color in this figure legend, the reader is referred to the web version of this article.)

was then shifted by 100 events to calculate the successive B- and H-values of the next window. The error bars show the 95% confidence intervals. We have previously shown that the H-values fluctuate in the opposite direction to the variation in B [21]. While the value of B usually increases following a large avalanche, the value of H usually decreases. The H value then increases prior to the next large avalanche, while the B value decreases.

Here, we systematically explore the correlation coefficients between B and H by utilizing different window lengths. Fig. 2 shows the correlation coefficients between B- and H-values for different window lengths (from 100 to 4000) for four LRCS models with grid sizes of 50 by 50, 100 by 100, 200 by 200 and 400 by 400. This figure shows that the relationship between the two exponents (H and B) is strongly dependent upon the window length. When the window length is too short, so that relevant events may be divided into different temporal windows, the correlation between B and H may be weak, as indicated by small absolute values of the correlation coefficients. On the other hand, when the window length is long, it is likely to include irrelevant events within a single calculation window. Consequently, the absolute values of the correlation coefficients between B and H may again be small. However, the negative correlation between B and H can be clearly seen when an appropriate window length is employed for various sandpiles.

Note that the horizontal axis in Fig. 2 corresponds to the rescaled window length. To consider the finite-size effect, we calculated the correlation coefficients between B- and H-values for different system sizes L. We then rescaled the original window lengths for LRCS models of different system sizes by $L^{1.5}$. When the rescaled window length is about 0.3, the relationship between B- and H-values shows the most significant negative correlation, with correlation coefficients ranging from -0.4 to -0.8, for L increasing from 50 to 400 (Fig. 2). As L increases, the significance of the negative correlation becomes stronger. The L-independence of the relationship between B and H (i.e., the same behavior is observed for different system sizes L) suggests the negative correlation observed here cannot be attributed to the finite-size effect [12] and can be considered a genuine characteristic of the relationship between B and H in the LRCS model.

4. Relationship between *B*- and *H*-values for avalanches in real seismicity

It is interesting whether this negative correlation exists between B and H for real earthquake data. To address this question, we analyzed the earthquake catalog of the Taiwan Central Weather Bureau (CWB). The CWB earthquake catalog includes occurrence data for earthquakes that occurred in the area of Taiwan from 1995 through 2007 (Fig. 3). The frequency–magnitude distribution of earthquakes from the CWB catalog is shown in the inset of Fig. 3. The magnitude/size distribution of earthquakes with magnitudes greater than 2 fulfills the Gutenberg–Richter law well, as the b-value (i.e., the abovementioned power-law exponent B) of the Gutenberg–Richter law is about

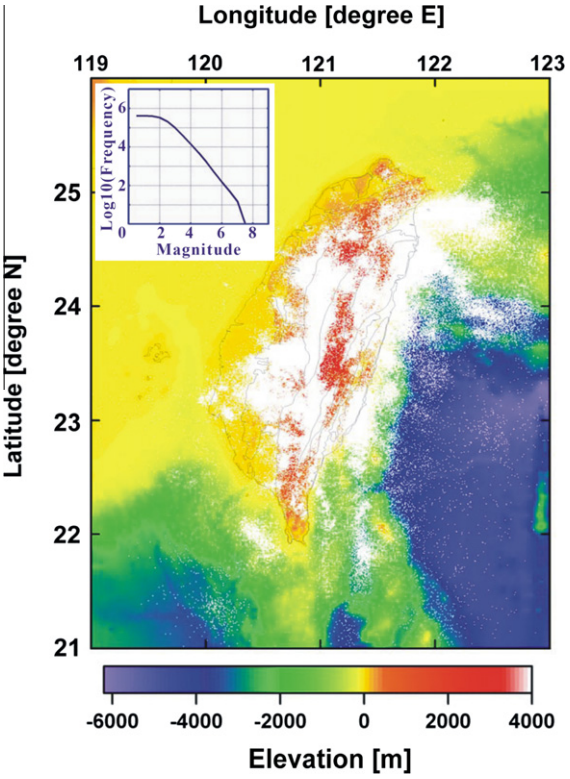

Fig. 3. Epicenters of earthquakes in the area of Taiwan included in this study. The map shows earthquakes with magnitudes greater than 2. The frequency–magnitude distribution of earthquakes in the CWB catalog is also shown (inset).

0.9. Note that the lowercase b is exclusively used in seismology to denote the scaling exponent of the power-law frequency–magnitude distribution (the Gutenberg–Richter law) of earthquakes. Therefore, to satisfy the requirement of a complete catalog, we considered magnitude 2 as the completeness magnitude throughout this study. In addition, to avoid the possibility of aftershock activity biasing the statistics, we removed aftershocks from the catalog by applying the de-clustering method of spatiotemporal double-links [37].

We first estimated the slip from the earthquake magnitude by using a first-order approximation without considering the details of rupture dynamics. In the elastic dislocation theory [17], a fault with a rupturing area A and a displacement offset δ can be represented by a force couple with a moment M_0 of $\mu\delta A$, where μ is the rigidity of the medium surrounding the rupture source. Statistically, the scaling relationship between the seismic moment and the fault area is $M_0 \sim A^{3/2}$ (e.g., Fig. 11 of [17]). Therefore, the average slip $\langle\delta\rangle$ of an event is simply proportional to the cubic root of the seismic moment, which we could directly convert from the local magnitude in the CWB catalog [35]. The Hurst exponent of the slip data was then calculated by R/S analysis. The b-value of the frequency–magnitude distribution of the earthquakes was fitted by a least-squares regression. Fig. 4 shows an example of the temporal variations in the b- and H-values for seismicity

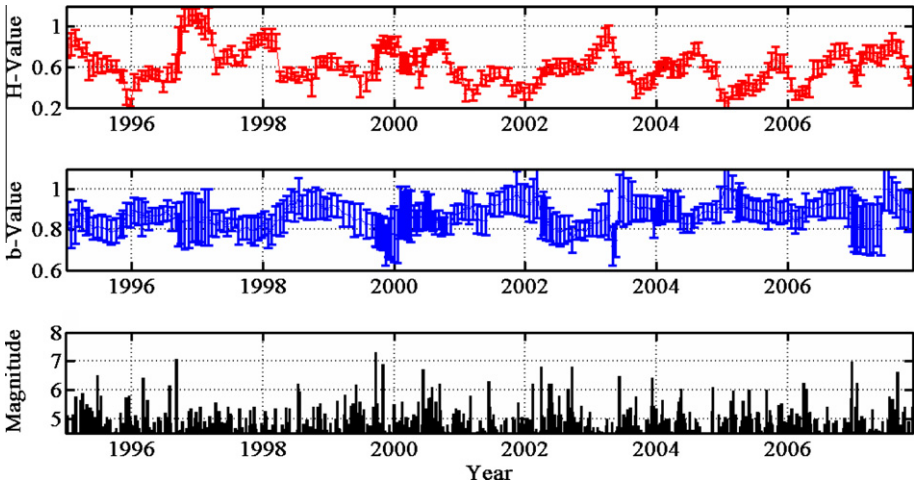

Fig. 4. Temporal variations in the values of b and H for real seismicity data in the CWB catalog from 1995 to 2007. Each point is calculated from a 5000-event window that is shifted by 500 events to calculate the successive b- and H-values of the next window.

data registered in the CWB catalog from 1995 to 2007. Each b and H value in Fig. 4 was calculated from 5000 events, and the window was shifted by 500 events to calculate the successive b- and H-values of the next window. Again, the variations of the b- and H-values clearly display a negative correlation (Fig. 5) and the correlation coefficient between b and H is about -0.5 (the solid red circle in Fig. 2). The lower plot of Fig. 4 also shows the occurrence of earthquakes with magnitudes greater than 4.5. The 20 September 1999, Mw 7.6 Chi-Chi earthquake is a good example with some kind of anomalous b- and H-values beforehand. As shown in Fig. 4, starting from the middle 1998 through the end of 1999 before the Chi-Chi event, we can see an interesting relationship with a decreasing trend in the b-values and an increasing trend in the H-values. Wu and Chiao [37] also found the precursory decrease in the b-values for the Chi-Chi earthquake. Since precursory phenomena before large earthquakes are highly complicated and sort of beyond the scope of the present study, we here focus on the relationship between b and H. Also shown in Fig. 2, the red circles indicate the transition of the relationship between b and H with different window lengths from 500 to 10,000 earthquakes for the calculations of b and H. The transition of the relationship between the b- and H-values for real seismicity data is essentially the same as that shown by the LRCS model.

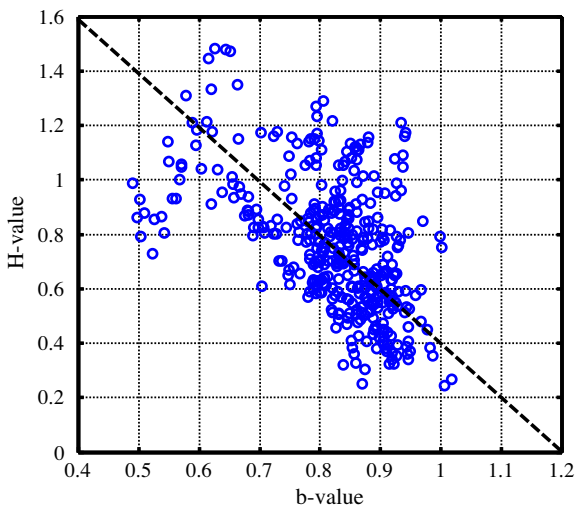

Fig. 5. Scatter plot for the b- and H-values calculated from real seismicity data of the CWB catalog.

5. Conclusion

The present study has important implications for earthquake statistics and stochastic processes. To seismologists, the negative correlation between the two scaling exponents (B and H) is fundamentally important for understanding earthquake statistics and rupturing processes [11,32,29]. Although the negative correlation between the two scaling exponents (B and H) has previously been suggested in some conceptual models of earthquake fault systems (e.g., [15]), it has been never demonstrated for natural seismicity data. Since its introduction, the BTW sandpile model has represented a conceptual paradigm of self-organized earthquake fault systems [5]. The original BTW sandpile models do not, however, show such a negative correlation [21]. To the contrary, the negative correlation between B and H exhibited in our LRCS model seems consistent with past studies of earthquake fault systems [11,15] and it can be also observed in the real earthquake data in Taiwan as presented in this paper. We also notice that some other studies had discussed the behavior of various scaling exponents for earthquake. Lapenna et al. [19] observed that a major earthquake is quite often preceded by opposite behaviors of the trends of the variance–time-curve exponent and the fractal dimension. Telesca et al. [30] also found a negative correlation between the time fractal exponent and the space fractal exponent that is related to the Gutenberg–Richter's b-value. Therefore, the

negative correlation between the time fractal exponent and b-value [30] would be consistent with what we found in the present paper.

An intuitive explanation of the negative correlation between B and H can be proposed. Large avalanches (small B) reshape the sandpile landscape, making it smoother so that there are fewer "traps" that could stop a future system-wide avalanche. As a result, H increases. In contrast, larger B values correspond to more small events, whose superposition results in higher-frequency noise in terms of the sandpile landscape and thus smaller H values. A similar conjecture has been proposed for the self-affine asperity model of Hallgass et al. [15] who observed that the scaling exponent of the frequency-size distribution depended on the roughness of the fault geometry, which is controlled by the Hurst exponent in the fractional Brownian fault profiles. In their numerical simulations (Fig. 4 in [15]), the observed negative correlation between the two scaling exponents was attributed to the self-affine nature of the considered fault ensembles. Notice that the scaling exponent B of the frequency-size distribution shares the geometric meaning of the fractal dimension [31,1]. Based on the self-affine traces of fractional Brownian motion Voss [33] has presented a relationship between the fractal dimension D and the Hurst exponent H, i.e. $D = 2 - H$, which then suggests the observed negative correlation between B and H here.

Acknowledgements

CCC is grateful for research support from both the National Science Council (ROC) and the Institute of Geophysics (NCU, ROC).

References

[1] Aki K. A probabilistic synthesis of precursor phenomena. In: Simpson DW, Richards PG, editors. Earthquake prediction: an international review. Maurice Ewing Ser., vol. 4. Washington, DC: American Geophysical Union; 1981. p. 566–74.
[2] De Arcangelis L, Herrmann H. Self-organized criticality on small world networks. Physica A 2002;308:545–9.
[3] Bak P, Tang C, Wiesenfeld K. Self-organized criticality: an explanation of the 1/f noise. Phys Rev Lett 1987;59:381–4.
[4] Bak P, Tang C, Wiesenfeld K. Self-organized criticality. Phys Rev A 1988;38:364–74.
[5] Bak P. How nature works: the science of self-organized criticality. New York: Copernicus Press; 1996.
[6] Castellaro S, Mulargia F. What criticality in cellular automata models of earthquakes? Geophys J Int 2002;150:483–93.
[7] Chen CC, Chiao LY, Lee YT, Cheng HW, Wu YM. Long-range connective sandpile models and its implication to seismicity evolution. Tectonophysics 2008;454:104–7.
[8] Chen CC, Lee YT, Chiao LY. Intermittent criticality in the long-range connective sandpile (LRCS) model. Phys Lett A 2008;372:4340–3.
[9] Christensen K, Olami Z. Sandpile models with and without an underlying spatial structure. Phys Rev E 1993;48:3361–72.
[10] Christensen K, Moloney NR. Complexity and criticality. London: Imperial College Press; 2005.
[11] Frankel A. High-frequency spectral fall off of earthquake, fractal dimension of complex rupture, b value, and the scaling of strength on faults. J Geophys Res 1991;96:6291–302.
[12] Garber A, Kantz H. Finite size effects on the statistics of extreme events in the BTW model. Eur Phys J B 2009;67:437–43.
[13] Goh KI, Lee DS, Kahng B, Kim D. Sandpile on scale-free networks. Phys Rev Lett 2003;91:148701/1–1/4.
[14] Goltz C, Bose M. Configurational entropy of critical earthquake populations. Geophys Res Lett 2002;29:51/1–4.
[15] Hallgass R, Loreto V, Mazzella O, Paladin G, Pietronero L. Earthquake statistics and fractal faults. Phys Rev E 1997;56:1346–56.
[16] Hughes D, Paczuski M. Large scale structures, symmetry, and universality in sandpiles. Phys Rev Lett 2002;88:054302/1–2/4.
[17] Kanamori H, Brodsky EE. The physics of earthquakes. Rep Prog Phys 2004;67:1429–96.
[18] Lahtinen J, Kertész J, Kaski K. Sandpiles on Watts–Strogatz type small-worlds. Physica A 2005;349:535–47.
[19] Lapenna V, Macchiato M, Telesca L. 1/f^{β} fluctuations and self-similarity in earthquake dynamics: observational evidences in southern Italy. Phys Earth Planet Int 1998;106:115–27.
[20] Lee YT, Chen CC, Chang YF, Chiao LY. Precursory phenomena associated with large avalanches in the long-range connective sandpile (LRCS) model. Physica A 2008;387:5263–70.
[21] Lee YT, Chen CC, Hasumi T, Hsu HL. Precursory phenomena associated with large avalanches in the long-range connective sandpile model II: an implication to the relation between the b-value and the Hurst exponent in seismicity. Geophys Res Lett 2009;36:L02308. doi:10.1029/2008GL036548.
[22] Lise S, Jensen HJ. Transitions in nonconserving models of self-organized criticality. Phys Rev Lett 1996;76:2326–9.
[23] Main IG, Al-Kindy FH. Entropy, energy, and proximity to criticality in global earthquake populations. Geophys Res Lett 2002;29:1121. doi:10.1029/2001GL014078.
[24] Manna SS. Two-state model of self-organized criticality. J Phys A: Math Gen 1991;24:363–9.
[25] Rundle JB, Klein W, Gross S. Physical basis for statistical patterns in complex earthquake populations: models, predictions and tests. Pure Appl Geophys 1999;155:575–607.
[26] Rundle JB, Klein W, Turcotte DL, Malamud BD. Precursory seismic activation and critical-point phenomena. Pure Appl Geophys 2000;157:2165–82.
[27] Sammis CG, Smith SW. Seismic cycles and the evolution of automation models of finite fault networks. Pure Appl Geophys 1999;155:307–34.
[28] Tang CC, Peng Z, Chao K, Chen CH, Lin CH. Detecting low-frequency earthquakes within non-volcanic tremor in southern Taiwan triggered by the 2005 Mw 8.6 Nias earthquake. Geophys Res Lett 2010;37:L16307. doi:10.1029/2010GL043918.
[29] Telesca L, Cuomo V, Lapenna V, Macchiato M. A new approach to investigate the correlation between geoelectrical time fluctuations and earthquakes in a seismic area of southern Italy. Geophys Res Lett 2001;28:4375–8. doi:10.1029/2001GL013467.
[30] Telesca L, Cuomo V, Lapenna V, Macchiato M. Identifying space-time clustering properties of the 1983–1997 Irpinia-Basilicata (southern Italy) seismicity. Tectonophysics 2001;330:93–102.
[31] Turcotte DL. Fractals and chaos in geology and geophysics. New York: Cambridge University Press; 1992.
[32] Turcotte DL. Self-organized criticality. Rep Prog Phys 1999;62:1377–429.
[33] Voss RF. Random fractals: self-affinity in noise, music, mountain, and clouds. Physica D 1989;38:362–71.
[34] Wang C, Chia YP, Dreger D. Role of S waves and love waves in coseismic permeability enhancement. Geophys Res Lett 2009;36:L09404. doi:10.1029/2009GL037330.
[35] Wang JH. Magnitude scales and their relations for Taiwan earthquakes: a review. Terr Atmos Ocean Sci 1992;3:449–68.
[36] Watts DJ, Strogatz SH. Collective dynamics of 'small-world' networks. Nature 1998;393:440–2.
[37] Wu YM, Chiao LY. Seismic quiescence before the 1999 Chi-Chi, Taiwan Mw 7.6 earthquake. Bull Seism Soc Am 2006;96:321–7.